International Journal of Automotive Technology, Vol. 7, No. 5, pp. 527−534 (2006)

Copyright © 2006 KSAE
1229−9138/2006/029−02

OXIDATION CHARACTERISTICS OF PARTICULATE MATTER ON DIESEL WARM-UP CATALYTIC CONVERTER

B. C. CHOI[1)*], Y. B. YOON[2)], H. Y. KANG[2)] and M. T. LIM[1)]

[1)]School of Mechanical Systems Engineering, Chonnam National University, Guwangju 500-757, Korea
[2)]Graduate School of Chonnam National University, Guwangju 500-757, Korea

(Received 4 October 2005; Revised 19 May 2006)

ABSTRACT–Modern passenger cars with diesel engines are equipped with DOC (diesel oxidation catalyst) for the purpose of reducing HC and CO in the exhaust stream. Cold start exhaust emissions pose troubles here as on gasoline engine vehicles. As a result, some of the diesel passenger cars roll off todays the assembly lines with WCC (warm-up catalytic converter). Oxidation characteristics of the particulates in WCC is analyzed in this study by EEPS (engine exhaust particulate size spectrometer). The maximum number of PM is found to come out of WCC in sizes near 10nm when an HSDI diesel engine is operated under the conditions of high speed and medium to heavy load. When the temperature of the WCC exceeds 300°C, the number of PM smaller than 30 nm in diameter sharply increases upon passing through the WCC. Total mass of emitted PM gets reduced downstream of the WCC under low speed and light load conditions due to adsorption of PM onto the catalyst. Under conditions of high speed and medium to heavy load, the relatively large PM shrink or break into fine particles during oxidation process within the WCC, which results in more mass fraction of fine particles downstream of the WCC.

KEY WORDS : Diesel engine, WCC (warm-up catalytic converter), DOC (diesel oxidation catalyst), PM (particulate matter), PM oxidation

1. INTRODUCTION

Direct injection (DI) diesel engines have high power and low fuel consumption with high-pressure fuel injection systems. Modern light-duty diesel engines show not only high power and low fuel consumption, but also improved exhaust emissions, noise, and vibration. The high-pressure fuel injection plays an important role in reducing the particulates and nitrogen oxides (NOx), which have been the most critical problems of the diesel engines. The DI diesel engines claim over 50% market share of diesel engine equipped passenger cars sold in Europe (Lee, 2000; Choi, 2001a, 2001b; Hori, 2003). It is reported that common-rail fuel injection systems using higher pressure are able to further decrease NOx and PM (particulate matter) emissions. However, the fuel droplets from the high-pressure injectors are smaller than those from the conventional injectors, which seems related to nano-scale particulates that are emitted more from engines with the high-pressure common-rail systems. The nano-scale particulates inhaled into human lungs stay there for long time. They can develop to nuclei of lung cancer (Park, 2000; Yeo, 2002; Jeong and Yoon, 2002).

Diesel exhaust gas is a complicated mixture of organic and inorganic compounds that are in gas, liquid, or solid phase. Diesel particulates consist of agglomerate of solids; hydrocarbon (HC) and sulfate gases adsorbed by the solid. PM might be associated with some liquid droplets, condensed hydrocarbon components, and sulfate particles. The constituents of the exhaust PM are very complex, and detailed mechanism of their formation are not fully known (Barris, 1992; Vincent *et al.*, 2003; Oh *et al.*, 2002).

Modern passenger cars with diesel engines are equipped with DOC (diesel oxidation catalyst) for the purpose of reducing HC and CO. Cold start exhaust emissions pose troubles here as in gasoline engine vehicles. This caused the WCC (warm-up catalytic converter) to be applied to some of the diesel passenger cars. In a previous study of the authors (Choi *et al.*, 2003; Choi *et al.*, 2001) PM conversion characteristics of a DOC was investigated. There was observed a trend of large scale particulates being partially oxidized to generate small particulates of smaller than 270 nm in diameter. The present study is an attempt to investigate the oxidation characteristics of particulates in a WCC for diesel passenger cars.

**Corresponding author.* e-mail: bcchoi@chonnam.ac.kr

2. EXPERIMENTAL SETUP AND PROCEDURES

2.1. Engine Exhaust Particulate Measurement

The EEPS (engine exhaust particulate size spectrometer) was developed by TSI (Johnson *et al.*, 2004) for analysis of the engine exhaust particulates. The EEPS uses a unique charging system and multiple electrometers to simultaneously receive signals from particles of all sizes. Signal data from the electrometer are processed in real time to output numbers of particulates that go through each of the 32 equally spaced channels for particles of different size. The EEPS spectrometer used in this study, specifications of which are shown in Table 1, is of a model designed for counting the submicrometer particles in the range of 5.6 to 560 nm in diameter.

2.2. Experimental Setup and Test Engine

Figure 1 represents the schematic diagram of the experimental apparatus. Specifications of the test engine are given in Table 2. The engine was tested for rated speed and maximum torque before the EEPS measurements to define the operating conditions that constitute the 15 mode test cycle shown in Figure 2. The engine dynamometer used was an eddy current dynamometer (Fuchino, ESP-600) capable of absorbing 440 kW. An exhaust gas analyzer made by HORIBA (Mexa-9100DEGR) was also used in the experiment. The measured concentrations of NOx and CO_2 were the basis for calculating the dilution ratio in measuring the particulates.

A dilution tunnel is made of steel pipe 2.6 m long and 0.12 m in diameter. The tunnel has a turbulence generator and a wake disk in the lead section to aid the branched exhaust gas to mix in the main section with diluting fresh air drawn by an inverter-controlled blower from the ambient (Wei *et al.*, 2001; Kim, 1992). The tunnel and the branched exhaust gas line of stainless steel (diameter 12 mm) are electrically heated and thermally insulated to maintain at 300°C. The fuel was commercially available light diesel oil, which contained about 180 ppm of sulfur.

Table 1. Specifications of engine exhaust particle size spectrometer (EEPS).

Particle size range	5.6–560 nm
Particle size resolution	16 channel per decade (Total 32)
Electrometer channels	22
Inlet aerosol flow	10 L/min
Time resolution	0.1s
Inlet aerosol temperature	10–52°C
Operating temperature	0–40°C
Humidity	0–95%

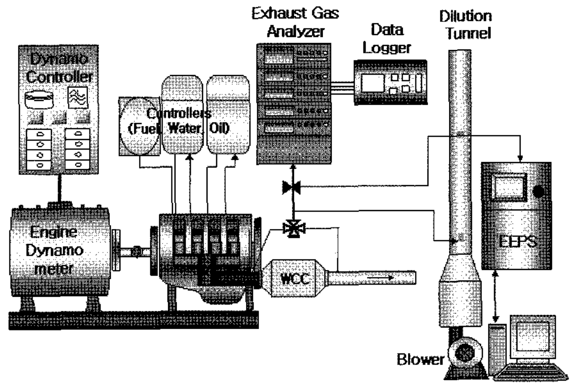

Figure 1. Schematic diagram of the experimental setup.

Table 2. Specifications of HSDI diesel engine.

Item	Specification
Engine type	4-stroke
Rated speed(rpm)	3200
Max. power (ps/rpm)	130 / 3200
Max. torque (kg.m/rpm)	33.5 / 2400
Air charging	Turbo-aftercooled
Bore×Stroke (mm)	97.1 dia.×98
Displacement (cc)	2903

The WCC tested in this experiment, 110 mm in diameter and 0.7 liter in volume, was prepared by Ordeg Co. The honeycomb type of monolithic substrate with cell density of 400 cpsi, was coated with gamma $-Al_2O_3$ and 2 different kinds of washcoat containing zeolites, and 2.5 g/*l* of platinum. The WCC was installed at some distance from the outlet of the turbo-charger, but the exhaust pipe leading to the WCC was completely insulated for fast activation.

2.3. Experimental Procedures

The 15 mode engine test cycle, employed in this study and shown in Figure 2, was originally constructed to represent typical operating patterns of diesel engines on heavy-duty vehicles in large cities in Korea, and is designated cycle for official determinations of exhaust emissions. (Choi *et al.*, 2001).

The temperatures of the cooling water, lubricant oil, and diesel fuel were respectively maintained at 85°C, 85°C and 40°C throughout the tests. All the measurements were made during the engine operation at each of the steady modes in D-15 cycle after the engine completely warmed up to those temperatures.

The sampling tube for the exhaust gas, connecting the engine exhaust pipe and the dilution tunnel, was heated to 300°C for minimal loss of particulates via condensation of water vapor and coagulation of the PM. A stainless

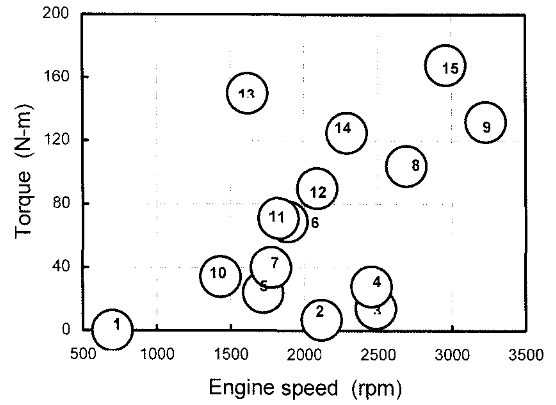

Figure 2. Engine operating conditions of 15-mode.

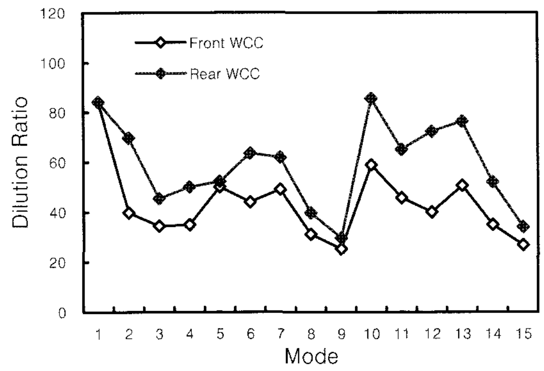

Figure 3. Dilution ratios by measured CO_2 concentration.

steel tube of 12 mm in diameter was used to minimize the Brownian loss, which may occur in the tube. The exhaust gas is diluted by the ambient air blown into the dilution tunnel before entering the EEPS at or below 50°C.

The concentration of CO_2 and NOx before and after the dilution were measured to determine the dilution ratio according to the following equation (1).

$$\text{Dilution ratio} = \frac{C_{undiluted} - C_{air}}{C_{diluted} - C_{air}} \quad (1)$$

Here, $C_{undiluted}$ and $C_{diluted}$ respectively represents the CO_2 or NOx concentration of the exhaust gas before and after the dilution, and C_{air} is the CO_2 or NOx concentration of the atmospheric air (Kim, 1992).

Numerical values of the dilution ratio calculated by this method were slightly different depending on whether CO_2 or NOx was used as tracing speises. The dilution ratio determined by using NOx concentration was chosen in this investigation. Considering that both particle number and mass of PM are proportional to the dilution ratio, the tracing gas must be carefully chosen for reasonable accuracy in determination of dilution ratio. Average values of the recorded signal over 2 minutes were taken for measured data at each mode of the 15-mode test cycle. The size distribution of PM were analyzed by determining the number of particles with diameters in each of the 12 subranges within total measuring range between 5.6 nm and 560 nm. The measurements were performed 2 times in each mode to confirm the data scatter.

3. EXPERIMENTAL RESULTS AND DISCUSSION

3.1. Dilution Ratio

Figure 3 shows the dilution ratio measured during the 15-mode test cycle. The dilution ratio in the rear of the WCC, calculated from the CO_2 concentration, are seen to be 30–80:1. The overall trends of the dilution ratio measured before and after the WCC look similar, although the dilution ratio is somewhat higher in the rear of the WCC due to the pressure difference existing at the sampling locations. The dilution ratio is different at each of the modes because the flow-rate of fresh air into the dilution tunnel was set constant, but the flow-rate of the engine exhaust gas varies with speed and load.

3.2. WCC Oxidation Performance

Figure 4 shows the exhaust gas temperature in the front of the WCC at each operating mode. The temperature in the front of the WCC is almost the same as in the rear of the WCC. Activity or conversion efficiency of the WCC depends on the exhaust gas temperature, which is seen to be over 100°C throughout the entire test cycle. The lowest temperature is 100°C at mode 1, while the highest temperature is 400°C at mode 9, where the engine is run at high speed and heavy load.

Figure 5 represents the conversion efficiencies of hydrocarbon (HC) and carbon monoxide (CO) of the WCC determined during the 15-mode test cycle depicted in Figure 2. Maximum conversion efficiency of the CO is 80% at mode 10. The HC conversion efficiency ranges from 60% to 80% in all of the modes except the modes 1, 2 and 3. These values are lower than usual values of WCC's on production vehicles. The main reason is the

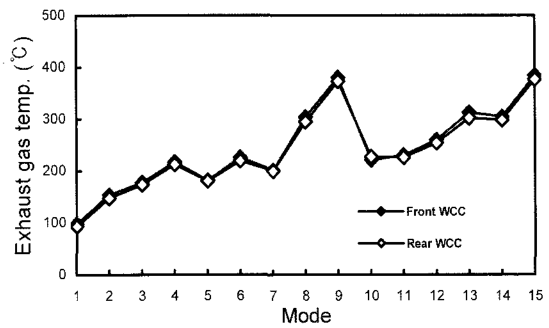

Figure 4. Exhaust gas temperatures of 15-mode.

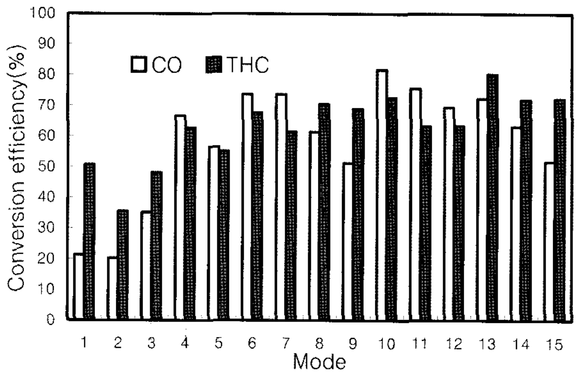

Figure 5. Conversion efficiencies of the WCC.

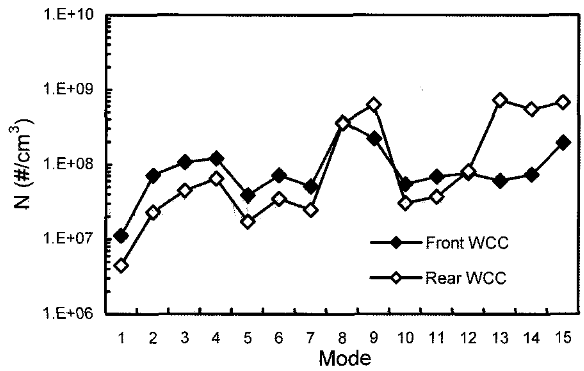

Figure 6. Total exhausted number of PM.

small volume (0.7 litter) of the present WCC, which push the space velocity (SV) in an unusually high range between 83,000 1/h(idling) and 385,000 1/h(mode 9). The exhaust gas temperature at modes 1 and 2 are 100 °C and 150°C respectively. These values are too low for the WCC to reach the state of catalytic activation.

The maximum gas temperature 400°C occurs at mode 9 where the conversion efficiencies of HC and CO are 52% and 70% respectively. In spite of the maximum gas temperature, conversion efficiencies are lower than at mode 13, probably because the SV of the catalyst is as high as 385,000 1/h due to high flowrate of the exhaust gas under the high speed and heavy load condition. And more CO is maybe attributed to the incomplete oxidation of HC and PM.

In case of mode 13 (SV=19,3000 1/h), although the exhaust gas temperature 310°C is lower than that of mode 9, the conversion efficiencies of HC and CO are the highest.

3.3. Particle Size Distribution

The number of PM with diameters ranging from 5.6 to 560 nm was measured. Figure 6 represents the total number of the PM in the front and rear of the WCC. The number of the PM emission of the HSDI diesel engine reached above 10^8 particle/cm^3 over 2200 rpm and medium range load conditions (in modes 3, 4, 8, 9, 14, 15). The total numbers of the PM in the rear of the WCC exceeded the number of the PM in the front of the WCC, namely at the engine out, in modes 8, 9, 12 to 15. And the total number of PM in the rear of the WCC decreased during low to medium engine speed and low load conditions in the modes 1 to 7, 10 and 11. The reduction of the PM number in modes 1 to 7 caused the surface of the WCC having wide distributions of fine and irregular pores, to absorb the PM.

Figure 7 shows the size distributions of particles in the engine-out exhaust gas during the steady operation modes. For modes 8, 9 and 15, each of the particle size distribution curves show two peaks: the first one (around 10 nm) in the nuclei mode, and the second one (around 100 nm) in the accumulation mode. These modes are supposed to superimpose to result in the bimodal shape (Stetter *et al.*, 2005). The particles in nuclei mode are formed by the nucleation of sulfuric acid during the process of dilution and cooling of hot exhaust (Khalek *et al.*, 2003). The maximum number of the PM particles having diameters of 10 nm is about 7×10^7 particle/cm^3.

From the test results in the same figure, the HSDI diesel engine operating in modes 8, 9 or 15, the conditions of high speed and medium to heavy load, are seen to emit the most particles in the size range of about 10 nm in diameter. For engine operation in other modes, the PM particles with diameters in the range from 40–50 nm show the greatest number.

Figure 8 presents the particle size distribution at the outlet of the WCC for each of the steady-state modes. In

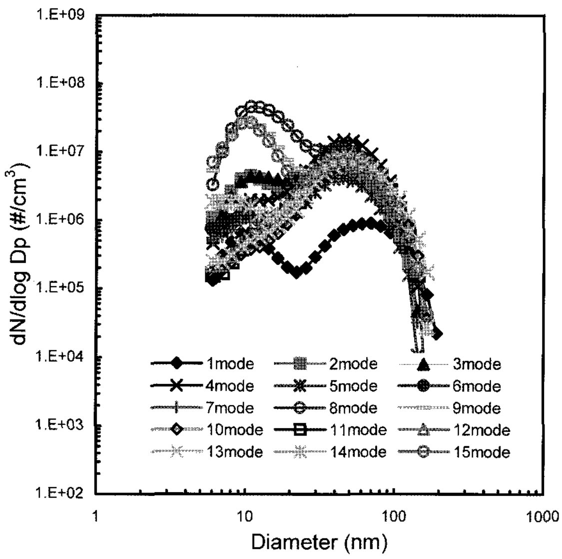

Figure 7. Particle number and size distribution of engine out emissions.

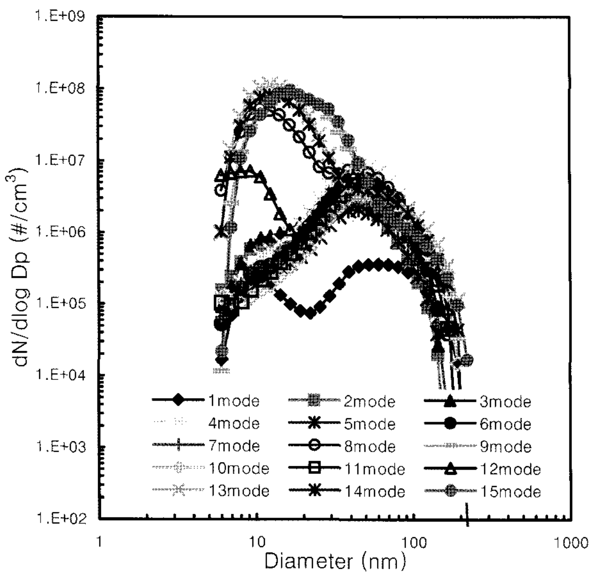

Figure 8. Particle size distribution in the rear of the WCC.

mode 9 and modes from 13 to 15, the number of particles in the nuclei mode around 10 nm in diameter increases upon passing through the WCC. In these modes, the number of 10–30 nm particles in the nuclei mode (Stetter *et al.*, 2005) ranges from 10^6 to 10^7 particle/cm^3 at the inlet of the WCC, but it increases to 10^8 particle/cm^3 at the outlet. And the number of particles over 30 nm in accumulation mode (Stetter *et al.*, 2005) decreases slightly. Large particles may capture some organic gas components on their surface, get partially oxidized at high temperature, then shrink to become small particles. It is also supposed that particles over 30 nm-diameter get partially oxidized and cracked on the catalyst surface. Water vapor concentration increases as organic fractions oxidize. Sulfur contained in fuel affects formation of nanoparticles via nucleation

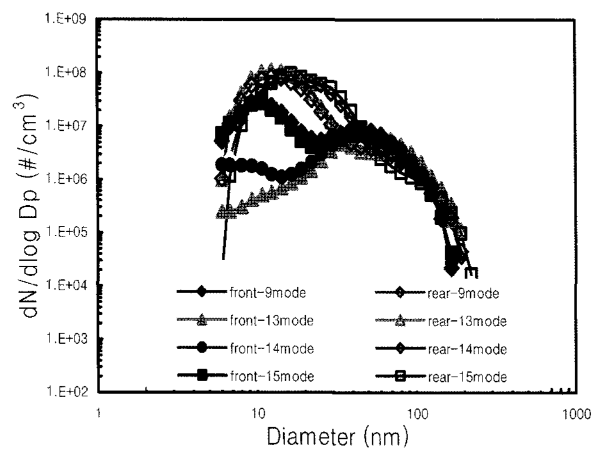

Figure 9. Comparison of particle size distribution at the front and the rear of the WCC in modes 9, 13, 14 and 15.

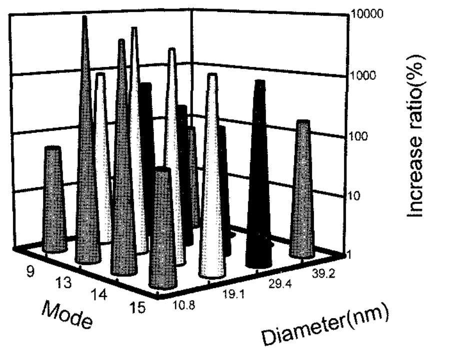

Figure 10. Ratio of number density for the size distribution in Figure 9.

of the sulfuric acid (Khalet *et al.*, 2003). The increased number of small particles in the nuclei mode includes droplets of water vapor and sulfuric oxides (Burtscher, 2005).

Figure 9 compares the particle size distributions at the front and rear of the WCC for engine operation modes 9, 13, 14 and 15 (conditions of high speed and medium to heavy load). The exhaust gas temperatures at the front of the WCC in modes 9 and 15 are about 400°C, and those in modes 13 and 14 are about 300°C. Under the engine operation conditions of high speed and medium to heavy load, where the exhaust gas temperature exceeds 300°C, the number of particles with diameter of less than 30 nm in the nuclei mode increase upon passing through WCC as was shown earlier in Figure 4.

Figure 10 shows the ratio of number density for the particles in the size range from 10 nm to 40 nm under the engine operation conditions of the modes 9, 13, 14 and 15. The ratio is defined as $(N_{out}-N_{in})/N_{in}\times100\%$, where N_{out} and N_{in} are respectively the particle number densities in the front and rear of the WCC. For the engine operation conditions of high speed and medium to heavy load, the ratio varies from 10% to 9,000% for the rane of particles from 10 nm to 40 nm in diameter. This indicates that the number of particles in nuclear regime increases within the WCC, while the number of larger particles over 40 nm in diameter decreases.

3.4. PM Mass Emission

The particulate mass emission was calculated using the measured particle size distribution and the PM density. Figure 11 shows the total mass emission of the particulates at the inlet and outlet of the WCC in each of the steady engine operation modes of the 15-mode test cycle. The total PM mass emission is less at the outlet than at the inlet in most modes except in modes 9 and 15. The decrease of total mass emission may be in part due to the adsorption of PM at the surface of WCC under the engine operation conditions of low to medium speed and load.

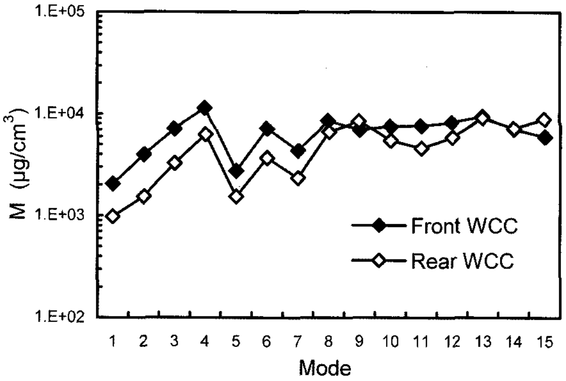

Figure 11. Total mass emission of PM.

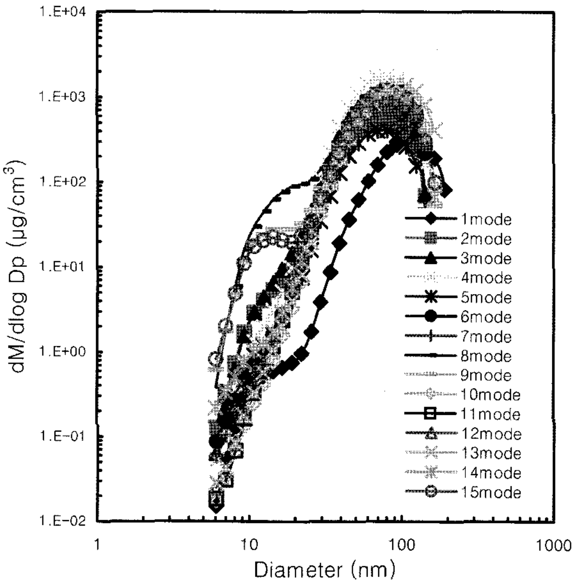

Figure 12. PM mass distributions in the front of the WCC.

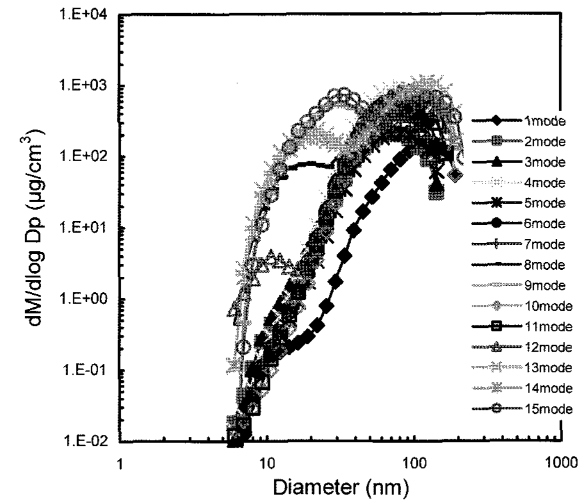

Figure 13. PM mass distributions in the rear of the WCC.

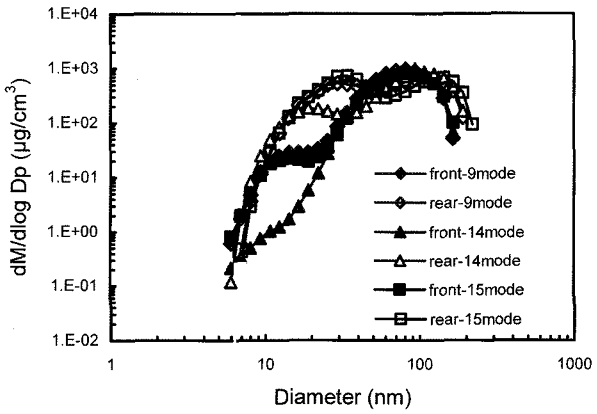

Figure 14. Comparison of the particle mass distribution in the front and rear of the WCC in modes 9, 14 and 15.

Increased total mass emission at the oulet of WCC in modes 9 and 15 may be then caused by the desorption of the adsorbed PM from the WCC surface in high temperature environment (400°C) during the engine operation at high speed and medium to heavy load.

Figure 12 depicts mass distribution of the engine-out particulates over their diameters. The maximum fraction of PM mass appears in the size range of 80–100 nm in general. Under the engine operating conditions of high speed and medium to heavy load such as modes 8, 9 and 15, secondary peaks appear in the size range of 10–20 nm. This bimodal distribution shares a similar tendency with the double peaks in Figure 7.

Figure 13 shows distribution of the PM mass over diameters downstream of the WCC. Maximum mass occurs in the size range of 70 to 120 nm, which is similar as in the front of the WCC. The total mass of the PM is less here when compared with that in front of the WCC. In the cases of mode 8, 9 and 13–15 of high speed and medium to heavy load, more mass of PM is found over the size range of 10–40 nm in the rear than in the front of the WCC. And mass of PM declines inside the WCC under low speed and medium load conditions due to adsorption onto the WCC, whereas the mass fraction of fine particles increases under the conditions of high speed and medium to heavy load due to desorption and partial oxidation of the large scale particles.

Distribution of particle mass in the front and rear of the WCC is compared in Figure 14 for modes 9, 14 and 15. More mass of particle is seen to exist over most part of the size range in the rear than in front of the WCC. It is apparent that mass of the particles with less than 40nm in diameter increases in all of these modes. This result indicates that, as was previously shown, large PM particles go through processes of partial oxidation, shrinking and

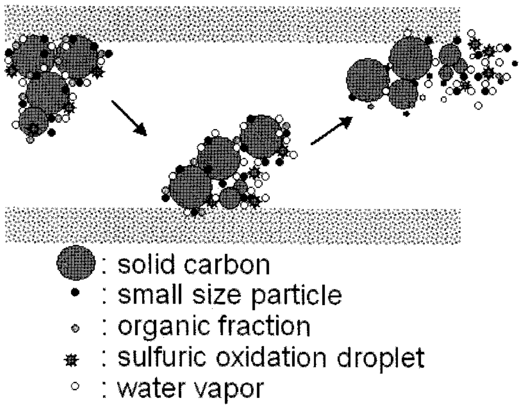

Figure 15. A model for PM oxidation on the catalyst.

cracking to become fine particles. The fine particle PM includes droplets of water vapor and sulfuric oxides (Burtscher, 2005). Sulfur contained in fuel affects nano-particle emissions via nucleation of sulfuric acid (Khalet *et al.*, 2003). The present study does not include the effects of sulfuric oxidation on nano size PM, which may warrant future research.

Based on the experimental findings above, a model for PM oxidation on the catalyst is postulated as shown in Figure 15. In the first step large scale carbonaceous particulates with high specific surface physically adsorbs vapor phase hydrocarbons onto their surface, (Barris, 1992; Choi, 2001) and then get themselves adsorbed on the catalyst of high specific surface area. In the next step, larger scale PM react on the catalyst with organic fractions, and get partially oxidized in high temperature conditions, shrink or break into mid scale particles in other conditions. Water vapor concentration increases due to oxidation of the organic fractions. Sulfur contained in fuel affects nanoparticle emissions via nucleation of sulfuric acid (Khalet *et al.*, 2003). The mid and small scale particles finally depart the catalyst including droplets of sulfuric oxidides and water vapor.

4. CONCLUSIONS

The characteristics of PM emitted from an HSDI diesel engine and their oxidation in a WCC are experimentally investigated under the engine operating conditions of 15-mode test cycle. The results of the study are summarized as follows:

(1) When the HSDI diesel engine with WCC operates under conditions of high speed and medium to heavy load, maximum number of PM are emitted around size of 10 nm in diameter.
(2) When the temperature of the WCC exceeds 300°C with the engine operating under conditions of high speed and medium to heavy load, the number of PM smaller than 30 nm in diameter increases during passage of the WCC by a multiplication factor of 0.1–9.
(3) Mass fraction of PM with diameters between 10–30 nm increases during passage of the WCC under engine operating conditions of high speed and medium to heavy load. Maximum fraction of mass is located around a size range of PM between 50–80 nm in diameter.
(4) Total mass of emitted PM is reduced by the WCC via adsorption onto the catalyst under engine operating conditions of low speed and light load. And under conditions of high speed and medium to heavy load, large PM seem to shrink or break into fine particles during oxidation inside the WCC. Mass fraction of fine PM is found larger after the WCC than before over the size range of 10–40 nm in diameter. The fine particulates may include water vapor and droplets of sulfuric oxidides.

ACKNOWLEDGEMENT–This work is part of the project "Development of Near Zero Emission Technology for Future Vehicle" and we are grateful for its financial support.

REFERENCES

Barris, M. A. (1992). Development of diesel exhaust catalytic converter muffler. *SAE Paper No.* 920369.

Burtscher, H. (2005). Physical characterization of particulate emissions from diesel engines: a review. *J. Aerosol Science* **36, 7,** 896–932.

Choi, B. C. (2001a). *Technologies for Emission Aftertreatment.* Baro Publishing Co.. Gwangju. Korea. 300–303.

Choi, K. H. (2001b). What will be the Future of HSDI Diesel Engines?. *J. Korean Society of Automotive Engineers* **23, 1,** 43–53.

Choi, B. C., Jung, P. S., Myung, K. J., Kim, B. S., Park, K. S., Park, C. G. and Lee, J. H. (2001). A study on evaluation of diesel oxidation catalyst for automotive heavy-duty diesel engine. *J. Korean Society for Power System Engineering* **5, 2,** 13–21.

Choi, B. C. Jang, S. H. and Juhng, W. N. (2003). ELPI measurement of particulate matters from HSDI diesel engine with diesel oxidation catalyst. *SAE Paper No.* 2003-02-3159.

Hori, M. (2003). Prospect of future automobile technology toward the first half of 21st century. *J. Society of Automotive Engineers of Japan* **57, 1,** 23–28.

Jeong, Y. I. and Yoon, M. K. (2002). Trend of diesel particulate filter trap technology. *J. Korean Society of Automotive Engineers* **24, 1,** 39–43.

Johnson, T., Caldow, R. A., Pocher, Mirmem, A. and Kittelson, D. (2004). A new electrical mobility particle sizer spectrometer for engine exhaust particle measurements. *SAE Paper No.* 2004-01-1341.

Khalek, I. A., Spears, M. and Charmley, W. (2003). Particle size distribution from a heavy-duty diesel engine: Steady-state and transient emission measurement using two dilution systems and two fuels. *SAE Paper No.* 2003-01-0285.

Kim, S. H. (1992). Purification technologies of diesel engine emission. *Chemical Industry and Technology* **10, 2,** 76–87.

Lee, D. Y. (2000). Trend of diesel fuel injection system. *J. Korean Society of Automotive Engineers* **22, 5,** 53–56.

Oh, S. K., Baik, D. S. and Han, Y. C. (2002). Performance and exhaust gas characteristics on particulate filter trap. *Int. J. Automotive Technology* **3, 1,** 111–115.

Park, J. K. (2000). Brief descriptions of automobile catalysts and the state of the art. *J. Korean Society of Automotive Engineers* **22, 5,** 41–46.

Stetter, J. C., Foster, D. E. and Schauer, J. J. (2005). Modern diesel particulate matter measurements and the application of lessons learned to 2007 levels and beyond. *SAE Paper No.* 2005-01-0194.

Vincent, M. W., Richards, P. J. and Rigers, T. J. (2003). Effective particulates reduction in diesel engines through the use of fuel catalyzed particulate filters. *Int. J. Automotive Technology* **3, 1,** 1–8.

Wei, Q., Kittleson, D. B. and Watts, W. F. (2001). Single-stage dilution tunnel design. *SAE Paper No.* 2001-01-0207.

Yeo, G. K. (2002). Trends of automotive catalyst technologies for low emission vehicles. *J. Korean Society of Automotive Engineers* **24, 1,** 28–32.